Supplementary Information

Self-organization in water of well-defined amphiphilic poly(vinyl acetate)-*b*-poly(vinyl alcohol) diblock copolymers

Julien Muller,[a] Franck Marchandeau,[b] Bénédicte Prélot,[b] Jerzy Zajac,[b] Jean-Jacques Robin,[a] and Sophie Monge*[a]

Polymer characterization

Synthesis of CTA-Si

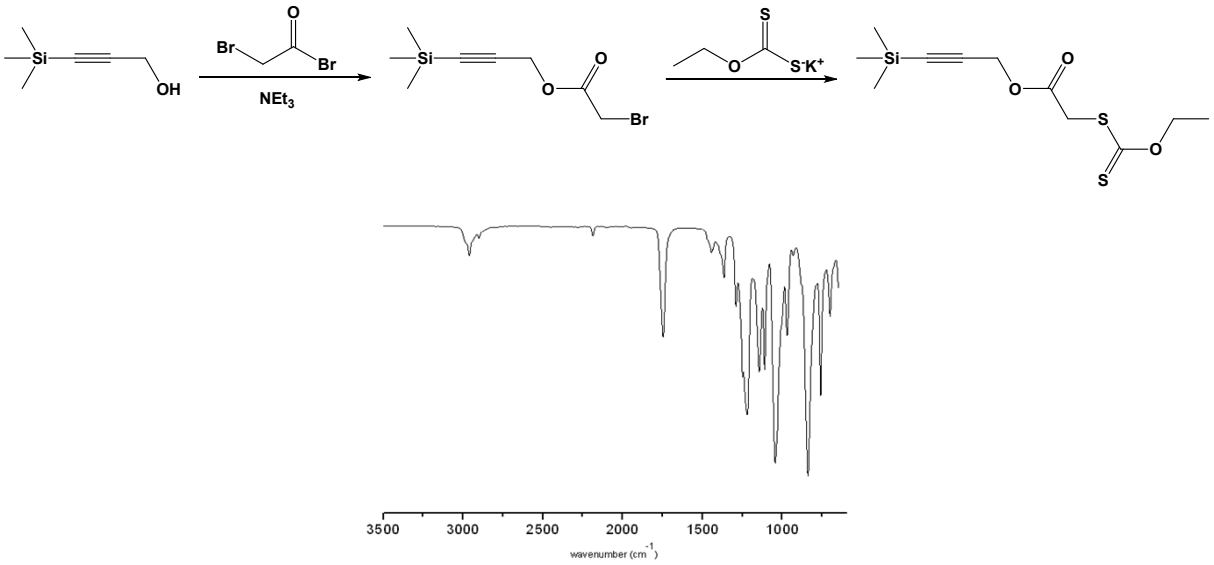

Fig. S1 Infrared spectrum of CTA-Si.

Synthesis of CTA-N_3

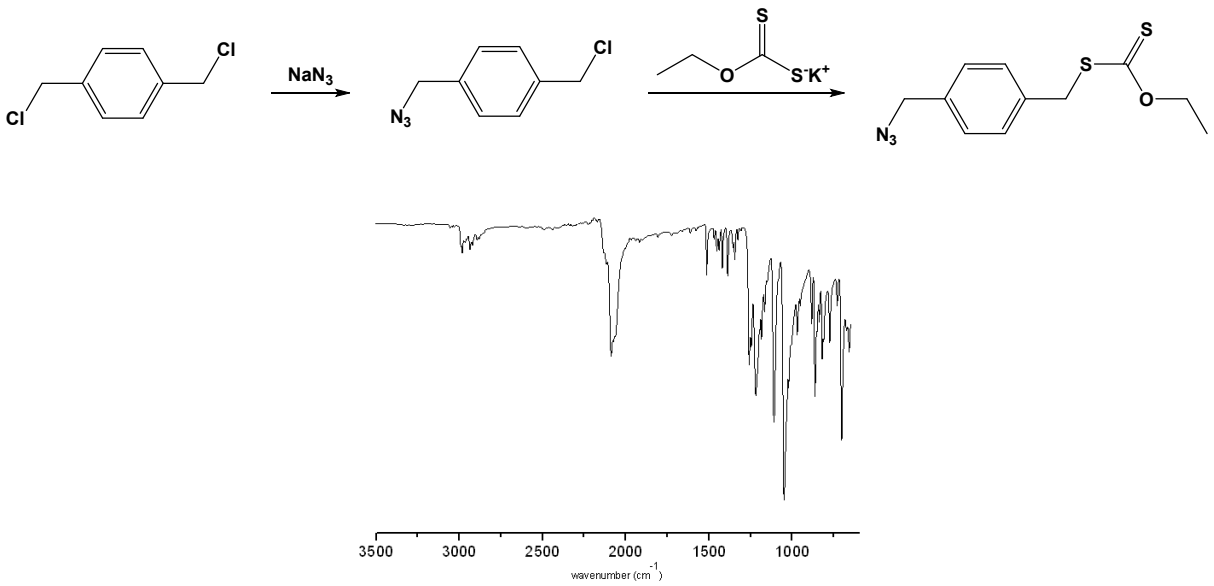

Fig. S2 Infrared spectrum of CTA-N_3.

Synthesis of PVA-N_3

Synthesis of the PVAc-N_3 homopolymers

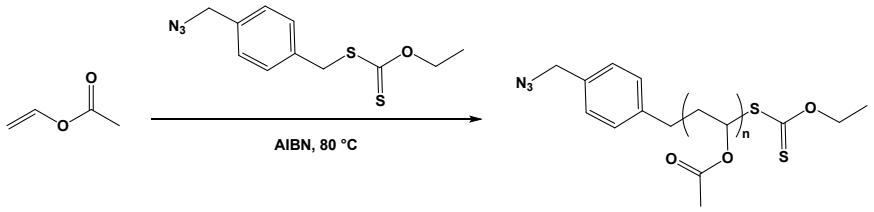

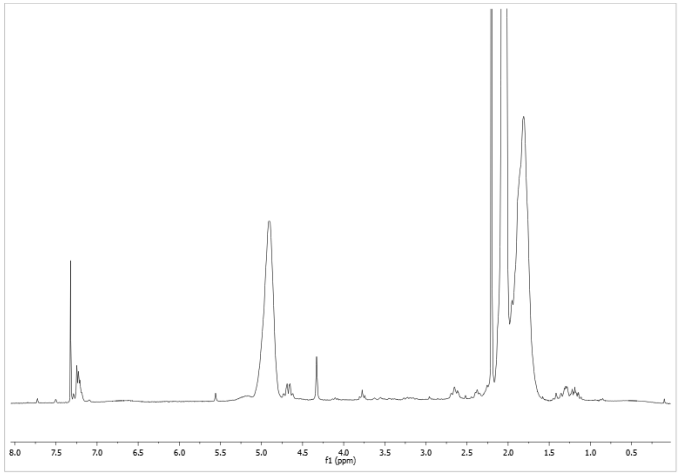

Fig. S3 ^{1}H NMR spectrum of PVAc-N_3 ($M_{n,\,NMR}$ = 4700 g·mol^{-1}) in $CDCl_3$.

Removal of xanthate function from PVAc-N_3

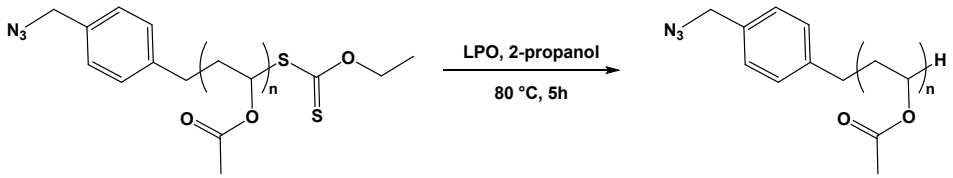

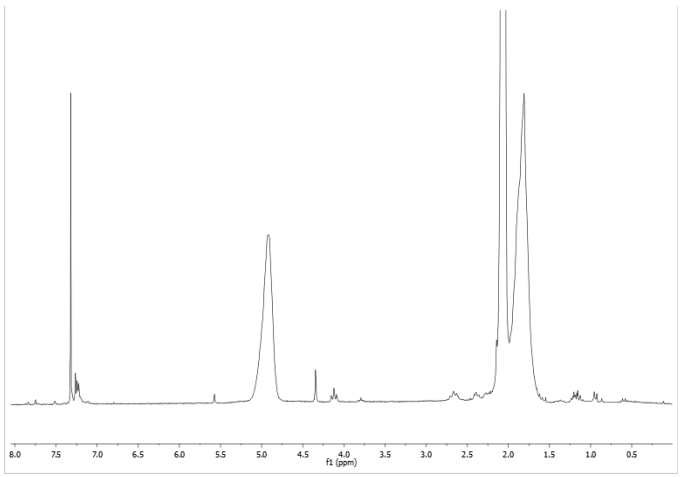

Fig. S4 ^{1}H NMR spectrum of PVAc-N_3 ($M_{n,\ NMR}$ = 4900 g·mol^{-1}) after the xanthate removal in $CDCl_3$.

Hydrolysis of PVAc-N_3

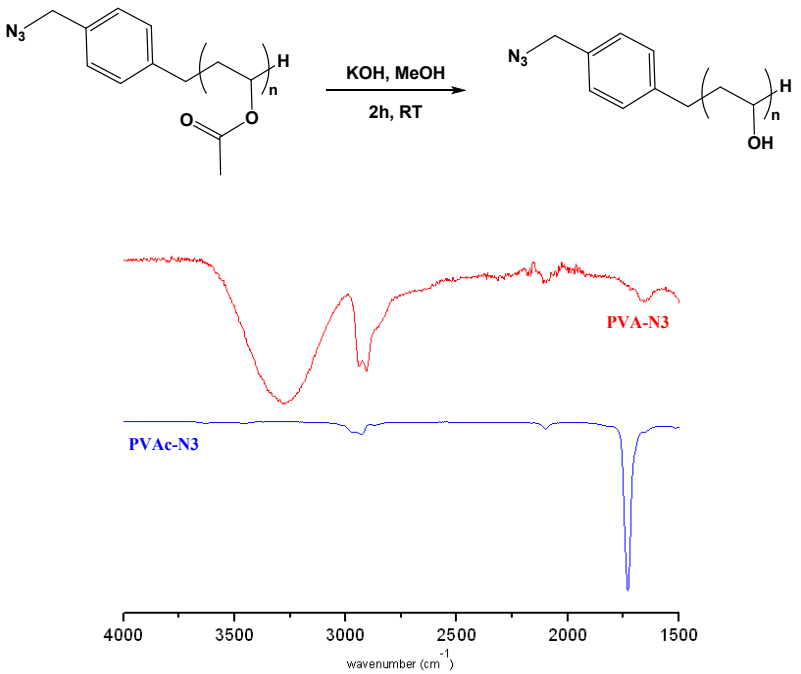

Fig. S5 IR spectra of PVAc-N_3 (blue signal, $M_{n,\,NMR}$= 5200 g·mol^{-1}, $Đ$ = 1.26) and PVA-N_3 (red signal, $M_{n,\,NMR}$ = 2900 g·mol^{-1}, $Đ$ = 1.25).

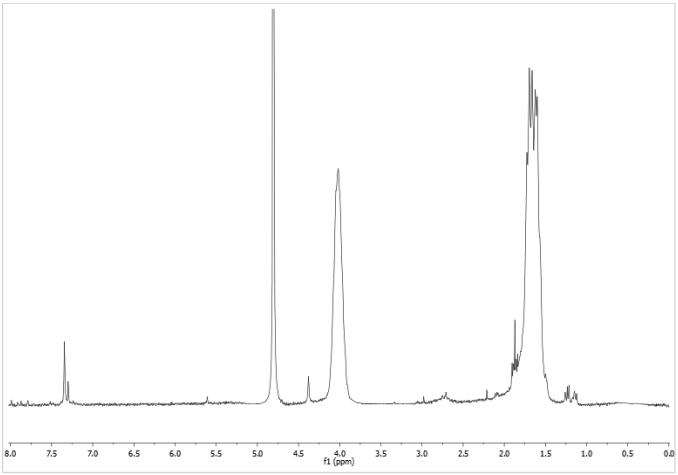

Fig. S6 ^{1}H NMR spectrum of PVA-N_3 ($M_{n,\,NMR}$ = 2900 g·mol^{-1}) in D_2O.

Synthesis of PVA-alkyne

Synthesis of the PVAc-Si homopolymers

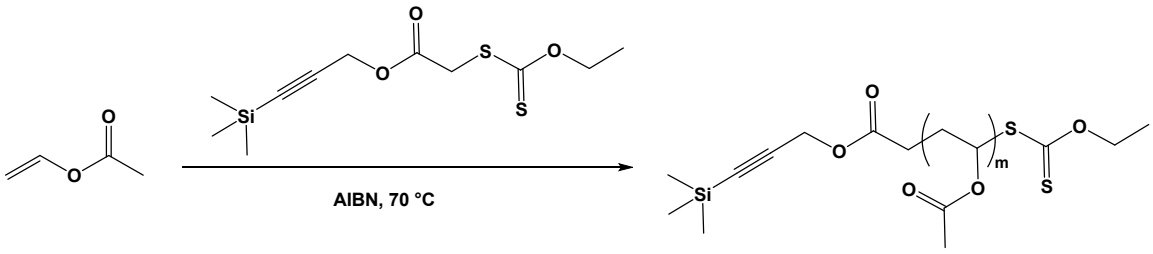

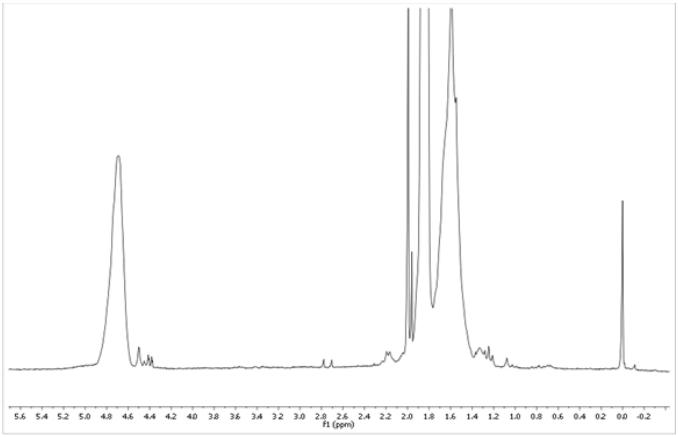

Fig. S7 ^{1}H NMR spectrum of PVAc-Si ($M_{n,\,NMR}$ = 10000 g·mol^{-1}) in $CDCl_3$.

PVAc-Si deprotection

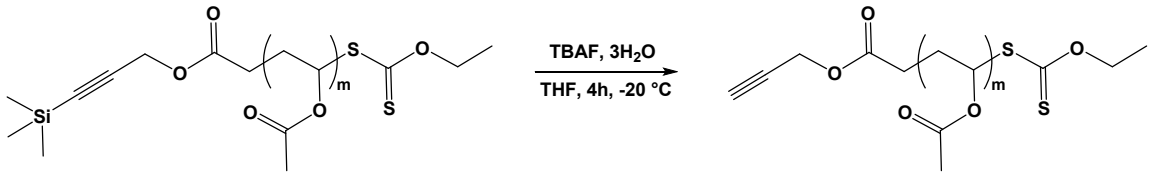

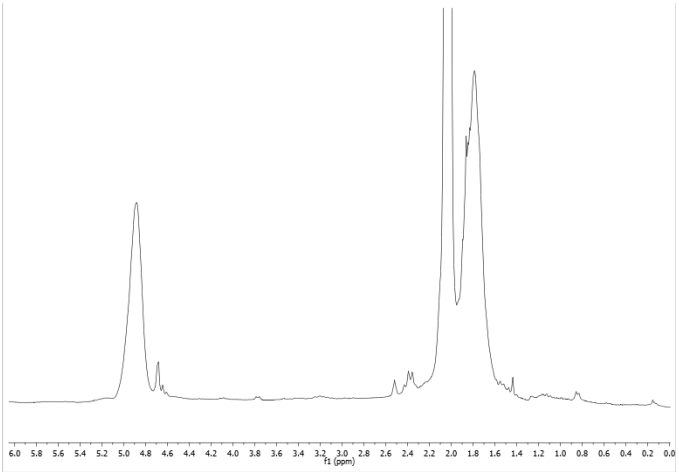

Fig. S8 ^{1}H NMR spectrum of PVAc-alkyne ($M_{n,\,NMR}$ = 5100 g·mol^{-1}) in $CDCl_3$.

PVAc-*b*-PVA copolymers synthesis

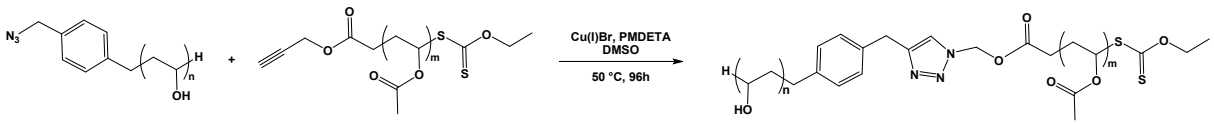

Copolymers Size Exclusion Chromatography (SEC) measurements

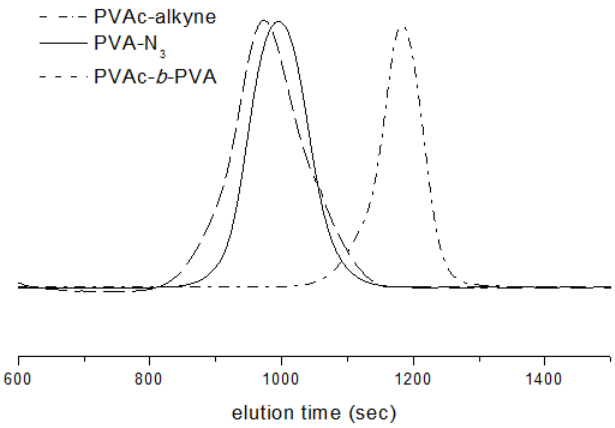

Fig. S9 SEC curves of $PVAc_{5100}$-alkyne (dash dot plot), PVA_{6200}-N_3 (solid plot) and $PVAc_{5100}$-*b*-PVA_{6200} (dash plot).

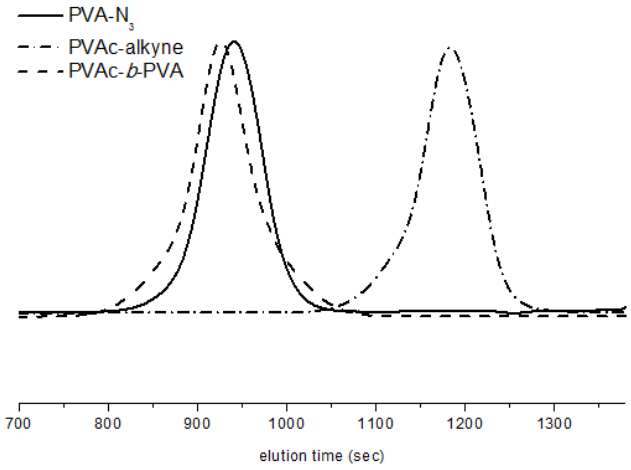

Fig. S10 SEC curves of $PVAc_{5100}$-alkyne (dash dot plot), PVA_{10000}-N_3 (solid plot) and $PVAc_{5100}$-*b*-PVA_{10000} (dash plot).

Physico-chemical properties of the PVAc-*b*-PVA

Determination of the particles size by DLS

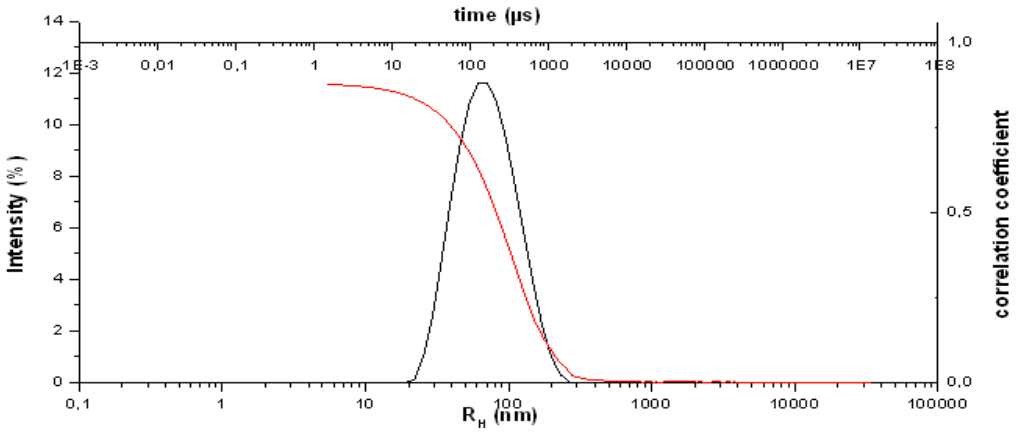

Fig. S11 Autocorrelation function (red) and size distribution (black) measured by DLS for a $PVAc_{5100}$-*b*-PVA_{6200} copolymer concentration of 0.1 $g \cdot L^{-1}$.

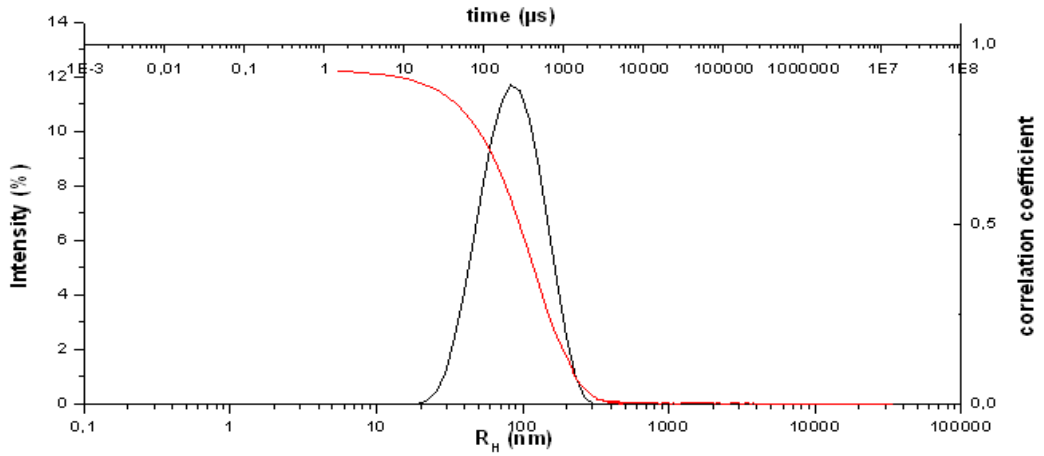

Fig. S12 Autocorrelation function (red) and size distribution (black) measured by DLS for a $PVAc_{5100}$-*b*-PVA_{10000} copolymer concentration of 0.1 $g \cdot L^{-1}$.

Determination of the CAC by pyrene fluorescence

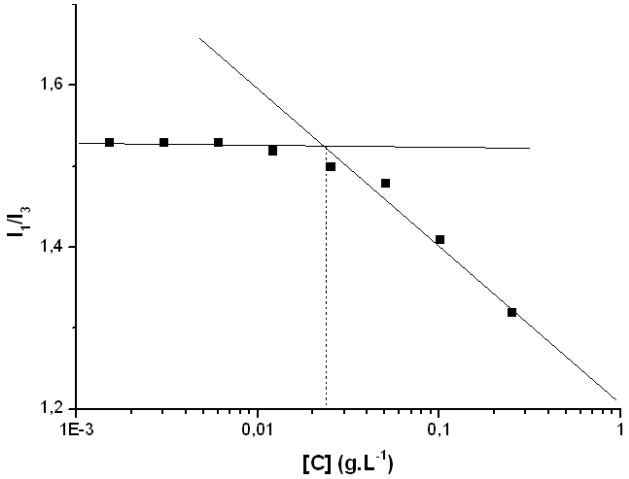

Fig. S13 Plot of the intensity ratio I_1/I_3 *versus* the polymer concentration (logarithmic scale) for $PVAc_{5100}$-*b*-PVA_{6200}.

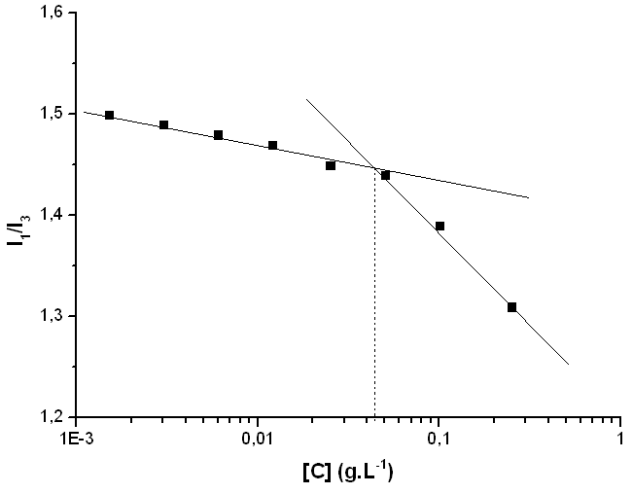

Fig. S14 Plot of the intensity ratio I_1/I_3 *versus* the polymer concentration (logarithmic scale) for $PVAc_{5100}$-*b*-PVA_{10000}.

Determination of the CAC by SLS

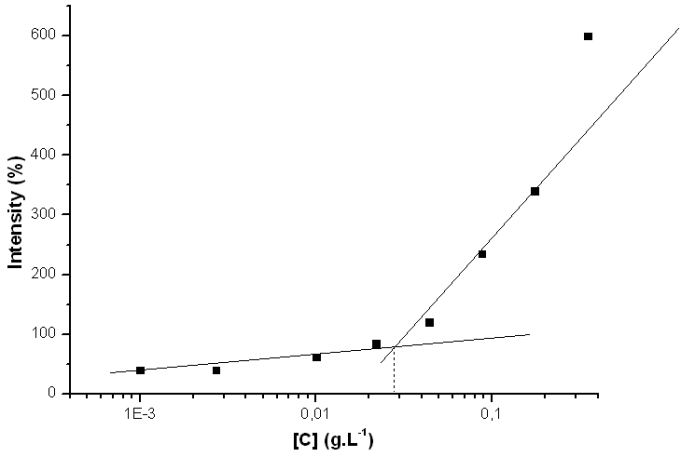

Fig. S15 Plot of the scattered intensity (%) as a function of the polymer concentration (logarithmic scale) for $PVAc_{5100}$-*b*-PVA_{6200}.

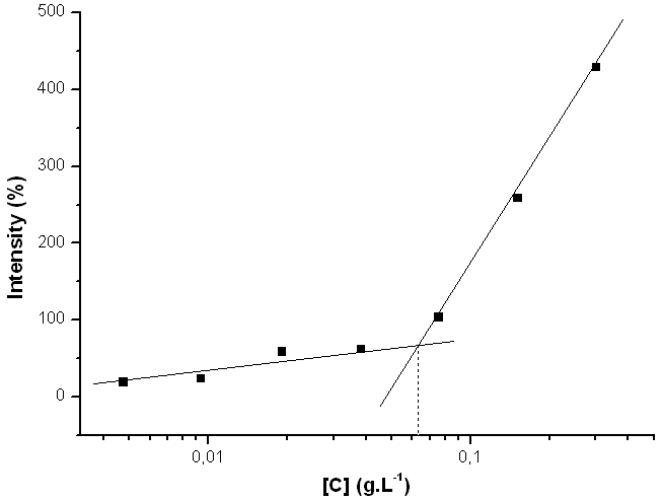

Fig. S16 Plot of the scattered intensity (%) as a function of the polymer concentration (logarithmic scale) for $PVAc_{5100}$-*b*-PVA_{10000}.

Determination of the CAC by isothermal microcalorimetry

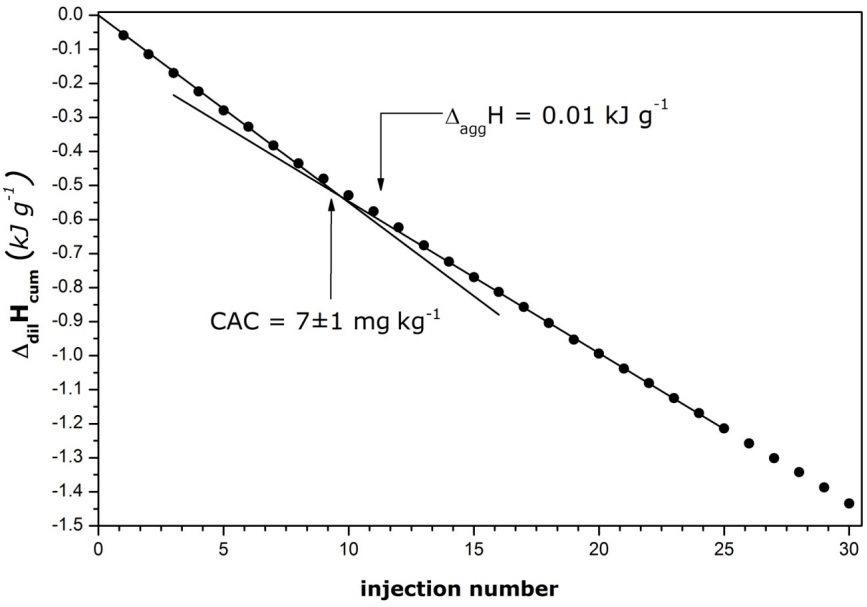

Fig. S17 Cumulative enthalpy of dilution for a concentrated stock solution of $PVAc_{5100}$-*b*-PVA_{6200} in pure H_2O per unit mass of copolymer at 303 K as a function of injection number.

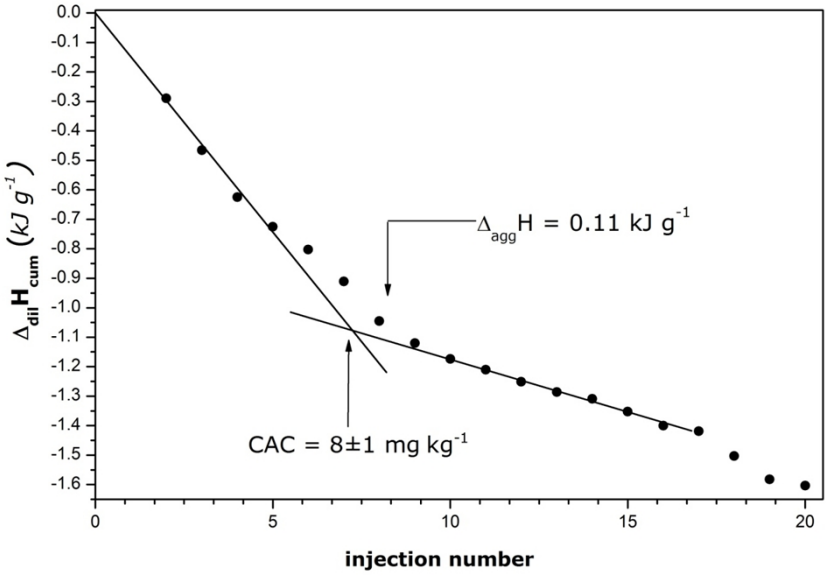

Fig. S18 Cumulative enthalpy of dilution for a concentrated stock solution of $PVAC_{5100}$-*b*-PVA_{10000} in pure H_2O per unit mass of the copolymer at 303 K as a function of injection number.